



**Italo-Russian Institute
of Education and Ecological Research**

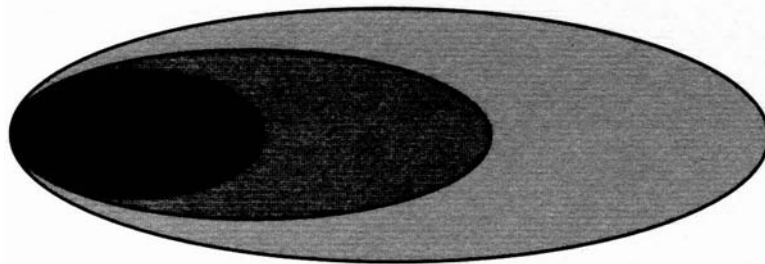


Università di Bari

2nd Symposium

PROTECTION OF GROUNDWATER FROM POLLUTION AND SEAWATER INTRUSION

Bari, September 27 - October 1, 1999



**VULNERABILITY MAPPING OF AN APULIAN
DEEP CARBONATE AQUIFER USING GIS**

Polemio M. & Ricchetti E.

VULNERABILITY MAPPING OF AN APULLAN DEEP CARBONATE AQUIFER USING GIS

M. Polemio¹, E. Ricchetti²

¹*CERIST - CNR, Bari*

²*Dipartimento di Geologia e Geofisica, Università di Bari*

Abstract

Computer techniques such as Geographic Information Systems are applied to the evaluation of the vulnerability of a deep carbonate aquifer.

The study area, of about 150 km², is located in the low Murgia Plateau (Apulia) and characterized by Mesozoic limestone and dolomite rocks of several thousand meters thickness. A wide aquifer resides in these carbonate rocks. Its groundwater flows toward the sea mainly under pressure and with maximum piezometric level of about 200 m a.s.l.. Due to their high quality, the water resources of this aquifer are particularly valuable for the local communities and therefore must be protected from pollution and inappropriate use.

The vulnerability map of the aquifer is an indispensable tool for the effective management of groundwater resources and to support environmental planning. Several approaches have been proposed by different authors to evaluate intrinsic vulnerability. Most of the methods for detailed vulnerability mapping are based on the integrated analysis of several variables using different algorithms. Geographic Information Systems are advanced computer tools for the analysis of georeferenced data in 2D and 3D and can be effectively applied to the implementation of evaluation models. In this study the SINTACS evaluation method was implemented in a GIS and a digital vulnerability map produced.

The different data taken into consideration in this analysis, such as depth to water; actual infiltration, pollution attenuation capacity of unsaturated zone, land cover; hydrogeological features of saturated aquifer; hydraulic conductivity, terrain slope, geology and geological structures, were georeferenced and converted into digital form. Each variable corresponds to a separate data layer made of graphic and attribute data.

The computerized multilayer analysis performed by the GIS is time effective and leads to more comprehensive and accurate results with better spatial resolution.

Introduction

Due to their geologic and hydrogeologic characteristics Apulian groundwater are very susceptible to pollution. Human activities that were developed in the last decade without comprehensive planning support may severely increase this risk locally. The location of any settlement that is a potential source of pollution has to be planned on the basis of detailed hydrogeological data and analysis, reported in a clear and straightforward form for use by decision-makers.

The intrinsic vulnerability map of aquifers is an effective information tool for these planning activities. This kind of maps quantitatively represents the sensitivity of any aquifer to receiving and transporting pollutants that may worsen groundwater quality (Civita, 1987; 1994; AA.VV., 1993).

In this paper we describe the use of Geographic Information Systems (GIS) to produce an intrinsic vulnerability map of a sample area in low Murgia Plateau, applying the SINTACS method (Civita & De Maio, 1997; Civita, 1994). This research takes place following the production of the vulnerability map for the same area using a traditional approach with a 500 m regular spaced grid (Cotecchia et al., 1999b).

Geological and hydrogeological setting

The study area is located in the wide hydrogeological unit of Murgia, made of Cretaceous carbonate rocks of platform environment. These deposits are mainly detritic limestone of the Apulian carbonate platform domain represented by the Calcare di Bari and Calcare di Altamura formations with a total thickness of more than 3000 m (Valduga, 1965; Ricchetti, 1975).

The outcropping rocks in the study area can be distinguished in the following three main geological units: Calcare di Bari; calcarenite deposits and alluvial deposits (fig. 1).

The Calcare di Bari formation is represented by a succession of micritic limestone in beddings of variable thickness, some of which are a few centimeters thick (chiancarelle), with some irregular sequences of dolomite limestone (Ricchetti, 1975; Ciaranfi et al., 1988).

The calcarenite deposits of Pleistocene age are locally overlaying the Mesozoic carbonate rocks in transgressive contact over abrasion flights. These calcarenites belong to the Calcarenite di Gravina formation, representing the opening of the Fossa Bradanica sedimentary cycle, and to marine terrace deposits transgressive over all the other formations. All the calcarenite deposits are bioclastic and generally massive with high variability in cementing grade.

Alluvial deposits of variable texture from coarse to fine, with a high content of residual deposit of red color (terra rossa), are present along the main drainage valleys (lame) and in the endoreic depression.

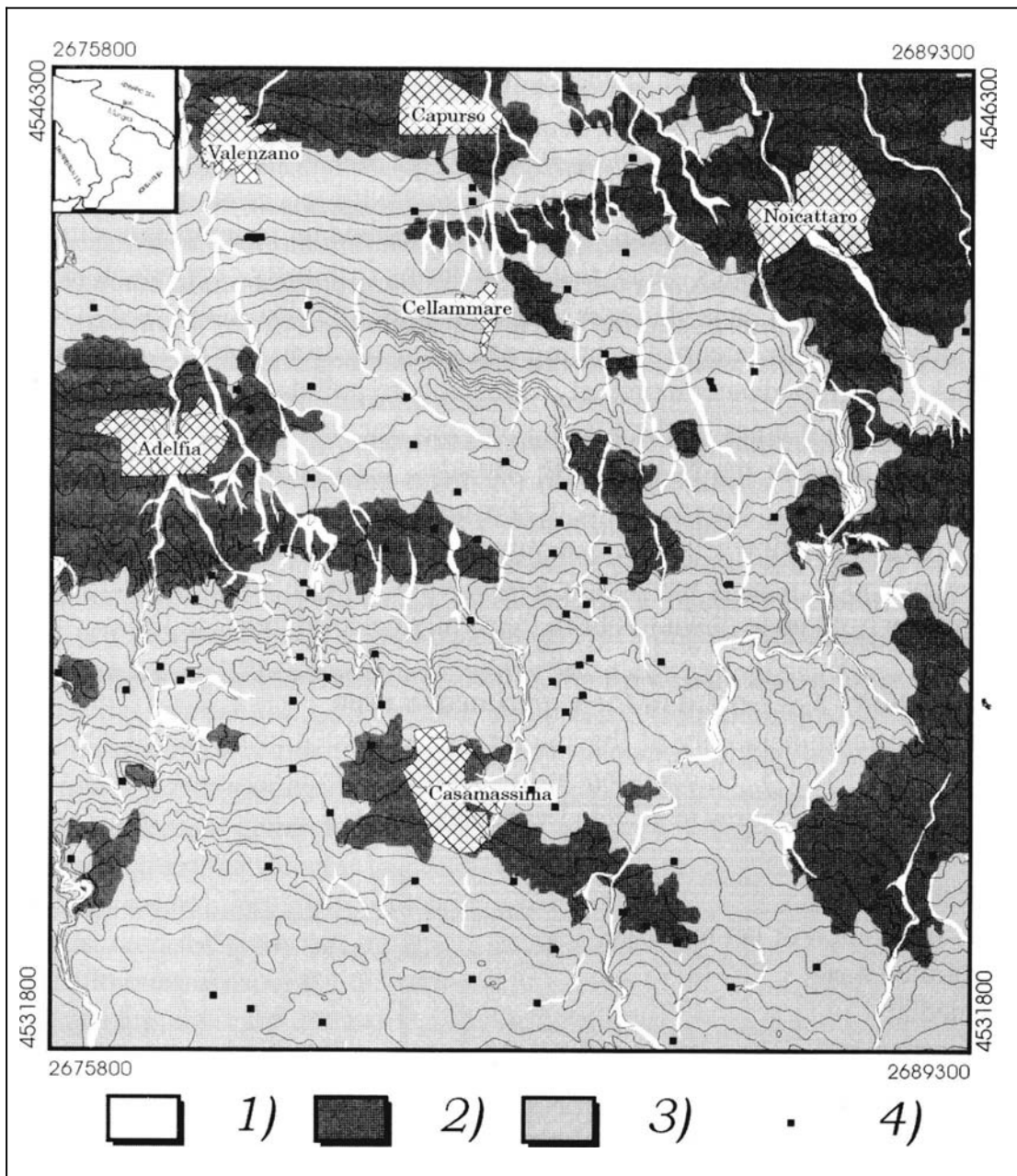


Fig. 1 - Geological map. Legend: 1) alluvial deposits; 2) calcarenite deposits; 3) Mesozoic limestones; 4) well.

The geological map of the area shown in fig. 1 is based on geological photointerpretation of stereoscopic aerial photographs with field checks in sample areas. This approach was used to produce a more detailed map than that of the official Geological Survey (scale 1:100,000) in a relatively short time.

In the Mesozoic carbonate rocks of Murgia lies a thick and large coastal aquifer, characterized by karstic phenomena and a highly variable fracture grade (Grassi, 1973;

Cotecchia, 1977). The hydraulic conductivity is anisotropy and uneven, with local high values due to karst and fractures. The sea level is the base level of groundwater flow. As a consequence the intruded seawater underlies fresh groundwater below sea level, owing to a difference in density. Over wide areas of Murgia the groundwater flows under pressure along several levels, at large depths of up to about 200-400 m below sea level in southeast Murgia.

The surface drainage is typical of karstic environments in temperate climates, with very low density and few gouges (lame) that flood during extremely exceptional intense rain. In the study area, the aquifer is characterized by several high hydraulic conductivity levels at different depths; due to intense fracturing and karst solution; these levels intersect each other and make the groundwater extremely vulnerable to pollutants coming from the terrain surface. In the high hill areas of the SE and SW the fractured levels occur less frequently than in the lower areas of the NW and NE. Besides, the hydraulic conductivity seems to increase in correlation with the fracturing in NW direction.

The groundwater flow velocity, determined by tracer tests, is generally high, between 0.5 and 4 m/day, and increasing toward low terrain areas. A remarkable vertical component of groundwater flow from up to down has been frequently detected in tested wells.

Vulnerability assessment of the experimental area

The intrinsic vulnerability of the aquifer was evaluated using the SINTACS method (Civita & De Maio, 1997). This approach divides the landscape into a grid with regularly spaced cells and assigns scores to selected variables for each cell. The variables used in this method are as follows:

S = depth to water;

I = actual infiltration or net recharge;

N = unsaturated zone;

T = soil media;

A = aquifer media;

C = hydraulic conductivity;

S = terrain slope;

A weight factor is associated to each variable according to its contribution to vulnerability. These weights are defined as functions of the local hydrogeological setting on the basis of many experimental evaluations in Italian test sites.

The intrinsic vulnerability for each cell is computed using the sum of the product of the scores and the weight of each variable.

Data set

The underground data used in this study were from the stratigraphy data of already existing wells and some wells especially drilled for this research. Besides cyclic surveys of the piezometric level, multiparametric logs (of temperature, electrical conductivity, pH, dissolved oxygen and oxidation-reduction potential) and measurements of groundwater flow

and vertical flow velocity have been carried out in about 200 drillholes (Cotecchia et al., 1999a).

,Topographic data were acquired from contour maps at 1:25,000 scale. To have a more comprehensive coverage of the study area these maps were digitized and linearly interpolated to produce a Digital Terrain Model. These data in digital format allow an easy quantitative analysis of terrain characteristics such as slope gradient and surface drainage pattern.

The climatic data, namely monthly rainfall and temperature, were acquired from the monitoring network of the Servizio Idrografico and Servizio Mareografico.

Data Analysis

All the data collected for this study were converted into digital format to implement in a Geographic Information System (GIS) for the vulnerability analysis. The uses of computer tools allows a more complex analysis with a finer spatial resolution than the traditional approach. Furthermore, GIS can easily manage data with high spatial variability. The analysis was accomplished on the basis of a raster grid with spatial resolution of 10 m.

The data and the analysis processes developed in this study to produce the intrinsic vulnerability map are schematically described in the flow chart shown in fig.2.

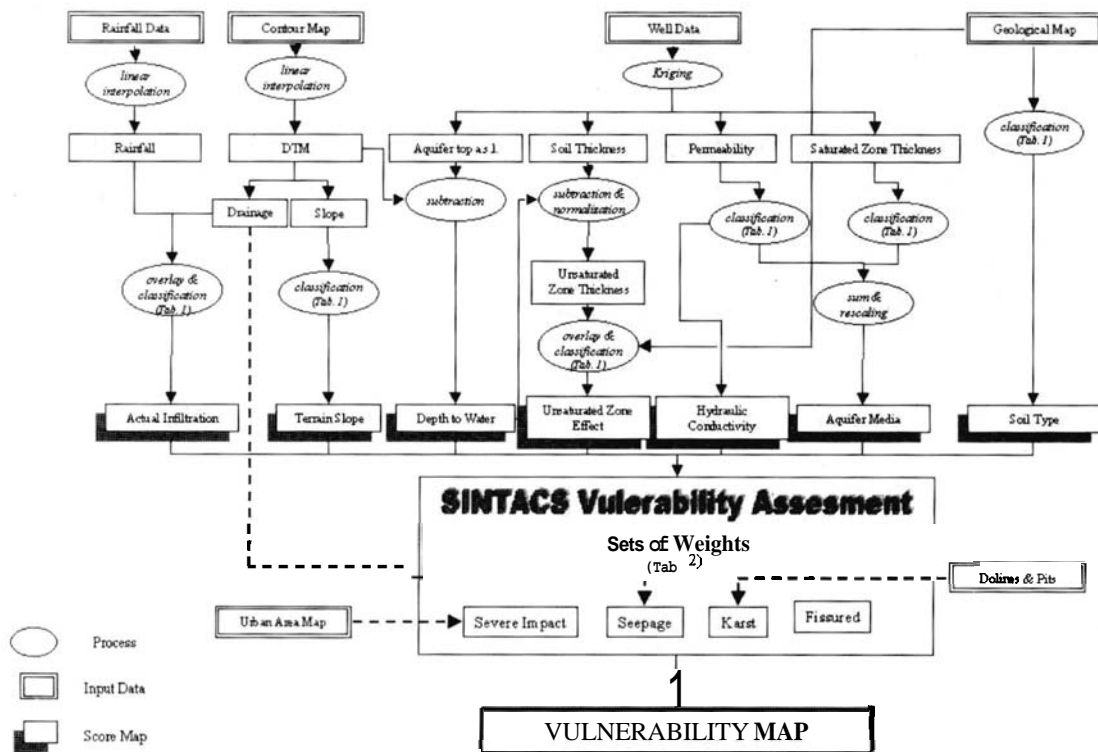


Fig. 2 - Schematic representation of vulnerability analysis process.

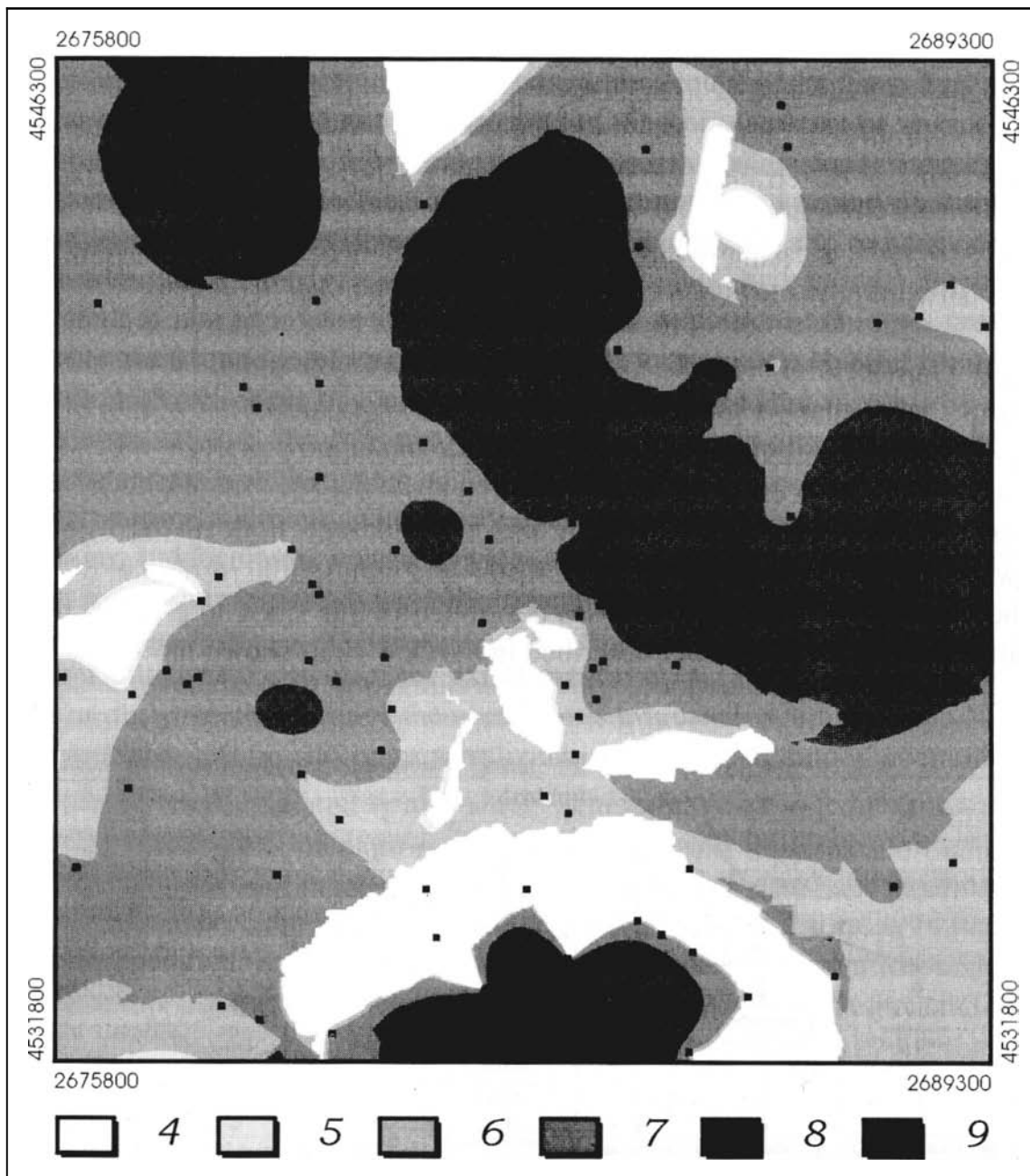


Fig. 3 - Score map of hydraulic conductivity (see tab. 1e).

All well data were input in a Data Base Management System (DBMS) linked to a point file reporting well locations in UTM coordinates. In order to produce maps of all the different variables measured in the drillholes and needed for computing the intrinsic vulnerability, well data were interpolated using a geostatistical approach. A semi-variogram for

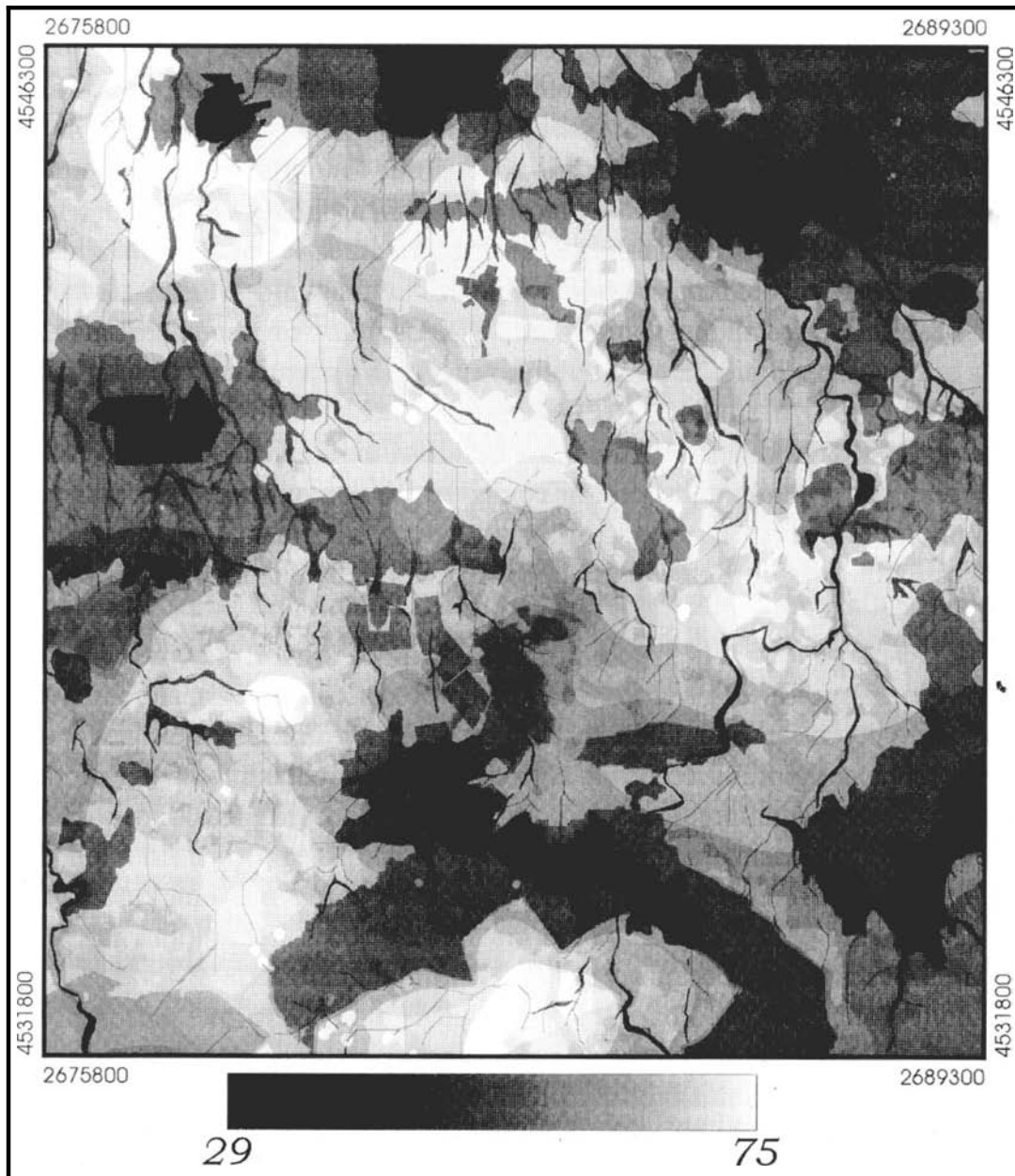


Fig. 4 - Vulnerability map (in percentage).

each variable was made from point data to define the interpolation function. Then several raster maps with 10 m resolution were computed for the different variables using kriging.

The geological map produced by aerial photointerpretation was digitized on-screen using the digital aerial photos as background. This vector map was input in the GIS using the same coordinate system as the other data

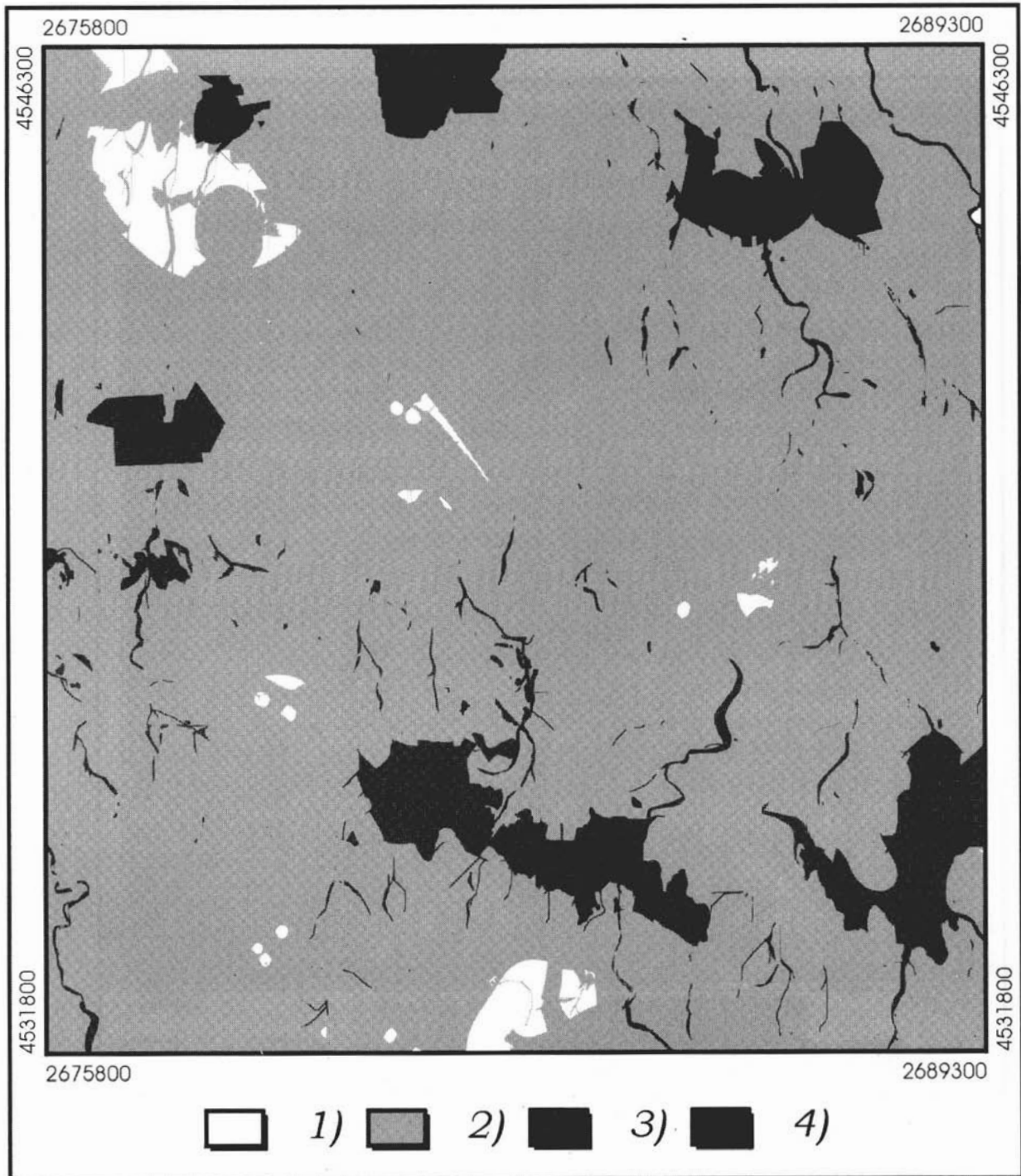


Fig. 5 - Vulnerability class map: 1) low (25%+35%); 2) medium (35%+50%); 3) high (50%+70%); 4) very high (70%+80%).

Since the groundwater flows under pressure, the depth of the aquifer top measured in the drillholes was used to produce the depth to water map. A spherical function with 10000 sill and 3000 range values was applied for interpolation by kriging. The depth to water is generally between 100 and 200 m over the study area, with large values of up to over 500 m

| <p>a)</p> <table border="1" style="width: 100%; border-collapse: collapse;"> <thead> <tr> <th>Depth to water</th> <th>Score</th> </tr> </thead> <tbody> <tr> <td>< 100 m</td> <td>3</td> </tr> <tr> <td>100÷200 m</td> <td>2</td> </tr> <tr> <td>> 200 m</td> <td>1</td> </tr> </tbody> </table> | Depth to water | Score | < 100 m | 3 | 100÷200 m | 2 | > 200 m | 1 | <p>b)</p> <table border="1" style="width: 100%; border-collapse: collapse;"> <thead> <tr> <th>Actual infiltration</th> <th>Score</th> </tr> </thead> <tbody> <tr> <td>< 90 mm/y</td> <td>4</td> </tr> <tr> <td>90÷110 mmly</td> <td>5</td> </tr> <tr> <td>■10÷130 mmly</td> <td>6</td> </tr> <tr> <td>130÷160 mm/y</td> <td>7</td> </tr> <tr> <td>> 160 mmly</td> <td>8</td> </tr> </tbody> </table> | Actual infiltration | Score | < 90 mm/y | 4 | 90÷110 mmly | 5 | ■10÷130 mmly | 6 | 130÷160 mm/y | 7 | > 160 mmly | 8 | | | | | | | | | | | | | | | | |
|--|------------------------|-------------------------------|----------------------|--------------|--|------------------------|---|----------------|--|----------------------------|--|-----------|--|---|----------------------|--------------|---|--|-------|------------|-------|---|---|-----------|---|---|---|-----------|---|--|---|--------|---|------------------------|----|--|--|
| Depth to water | Score | | | | | | | | | | | | | | | | | | | | | | | | | | | | | | | | | | | | |
| < 100 m | 3 | | | | | | | | | | | | | | | | | | | | | | | | | | | | | | | | | | | | |
| 100÷200 m | 2 | | | | | | | | | | | | | | | | | | | | | | | | | | | | | | | | | | | | |
| > 200 m | 1 | | | | | | | | | | | | | | | | | | | | | | | | | | | | | | | | | | | | |
| Actual infiltration | Score | | | | | | | | | | | | | | | | | | | | | | | | | | | | | | | | | | | | |
| < 90 mm/y | 4 | | | | | | | | | | | | | | | | | | | | | | | | | | | | | | | | | | | | |
| 90÷110 mmly | 5 | | | | | | | | | | | | | | | | | | | | | | | | | | | | | | | | | | | | |
| ■10÷130 mmly | 6 | | | | | | | | | | | | | | | | | | | | | | | | | | | | | | | | | | | | |
| 130÷160 mm/y | 7 | | | | | | | | | | | | | | | | | | | | | | | | | | | | | | | | | | | | |
| > 160 mmly | 8 | | | | | | | | | | | | | | | | | | | | | | | | | | | | | | | | | | | | |
| <p>c)</p> <table border="1" style="width: 100%; border-collapse: collapse;"> <thead> <tr> <th>Soil media (thickness)</th> <th>Score</th> </tr> </thead> <tbody> <tr> <td>Clay >100 cm</td> <td>2</td> </tr> <tr> <td>Loam to clay 50÷150 cm</td> <td>4</td> </tr> <tr> <td>Clay 0÷50 cm</td> <td>8</td> </tr> </tbody> </table> | | Soil media (thickness) | Score | Clay >100 cm | 2 | Loam to clay 50÷150 cm | 4 | Clay 0÷50 cm | 8 | | | | | | | | | | | | | | | | | | | | | | | | | | | | |
| Soil media (thickness) | Score | | | | | | | | | | | | | | | | | | | | | | | | | | | | | | | | | | | | |
| Clay >100 cm | 2 | | | | | | | | | | | | | | | | | | | | | | | | | | | | | | | | | | | | |
| Loam to clay 50÷150 cm | 4 | | | | | | | | | | | | | | | | | | | | | | | | | | | | | | | | | | | | |
| Clay 0÷50 cm | 8 | | | | | | | | | | | | | | | | | | | | | | | | | | | | | | | | | | | | |
| <p>d)</p> <table border="1" style="width: 100%; border-collapse: collapse;"> <thead> <tr> <th colspan="4">Aquifer media characteristics</th> </tr> <tr> <th>Hydraulic conductivity</th> <th>Score</th> <th>Saturated Zone</th> <th>Score</th> </tr> </thead> <tbody> <tr> <td>< 1 * 10⁻⁶ m/s</td> <td>4</td> <td>< 5 m</td> <td>1</td> </tr> <tr> <td>10⁻⁶ ÷ 10⁻⁵ m/s</td> <td>5</td> <td>5 ÷ 10 m</td> <td>2</td> </tr> <tr> <td>10⁻⁵ ÷ ■10⁻⁴ m/s</td> <td>6</td> <td>10 ÷ 20 m</td> <td>3</td> </tr> <tr> <td>10⁻⁴ ÷ 10⁻³ m/s</td> <td>7</td> <td>20 + 40 m</td> <td>4</td> </tr> <tr> <td>■10⁻³ ÷ ■10⁻² m/s</td> <td>8</td> <td>40 ÷ 80 m</td> <td>5</td> </tr> <tr> <td>■10⁻² ÷ 10⁻¹ m/s</td> <td>9</td> <td>> 80 m</td> <td>7</td> </tr> <tr> <td>> 10⁻¹ m/s</td> <td>10</td> <td></td> <td></td> </tr> </tbody> </table> | | Aquifer media characteristics | | | | Hydraulic conductivity | Score | Saturated Zone | Score | < 1 * 10 ⁻⁶ m/s | 4 | < 5 m | 1 | 10 ⁻⁶ ÷ 10 ⁻⁵ m/s | 5 | 5 ÷ 10 m | 2 | 10 ⁻⁵ ÷ ■10 ⁻⁴ m/s | 6 | 10 ÷ 20 m | 3 | 10 ⁻⁴ ÷ 10 ⁻³ m/s | 7 | 20 + 40 m | 4 | ■10 ⁻³ ÷ ■10 ⁻² m/s | 8 | 40 ÷ 80 m | 5 | ■10 ⁻² ÷ 10 ⁻¹ m/s | 9 | > 80 m | 7 | > 10 ⁻¹ m/s | 10 | | |
| Aquifer media characteristics | | | | | | | | | | | | | | | | | | | | | | | | | | | | | | | | | | | | | |
| Hydraulic conductivity | Score | Saturated Zone | Score | | | | | | | | | | | | | | | | | | | | | | | | | | | | | | | | | | |
| < 1 * 10 ⁻⁶ m/s | 4 | < 5 m | 1 | | | | | | | | | | | | | | | | | | | | | | | | | | | | | | | | | | |
| 10 ⁻⁶ ÷ 10 ⁻⁵ m/s | 5 | 5 ÷ 10 m | 2 | | | | | | | | | | | | | | | | | | | | | | | | | | | | | | | | | | |
| 10 ⁻⁵ ÷ ■10 ⁻⁴ m/s | 6 | 10 ÷ 20 m | 3 | | | | | | | | | | | | | | | | | | | | | | | | | | | | | | | | | | |
| 10 ⁻⁴ ÷ 10 ⁻³ m/s | 7 | 20 + 40 m | 4 | | | | | | | | | | | | | | | | | | | | | | | | | | | | | | | | | | |
| ■10 ⁻³ ÷ ■10 ⁻² m/s | 8 | 40 ÷ 80 m | 5 | | | | | | | | | | | | | | | | | | | | | | | | | | | | | | | | | | |
| ■10 ⁻² ÷ 10 ⁻¹ m/s | 9 | > 80 m | 7 | | | | | | | | | | | | | | | | | | | | | | | | | | | | | | | | | | |
| > 10 ⁻¹ m/s | 10 | | | | | | | | | | | | | | | | | | | | | | | | | | | | | | | | | | | | |
| <p>e)</p> <table border="1" style="width: 100%; border-collapse: collapse;"> <thead> <tr> <th>Hydraulic conductivity</th> <th>Score</th> </tr> </thead> <tbody> <tr> <td>10⁻⁶ m/s</td> <td>4</td> </tr> <tr> <td>■10⁻⁶ - 10⁻⁵ m/s</td> <td>5</td> </tr> <tr> <td>10⁻⁵ ÷ 10⁻⁴ m/s</td> <td>6</td> </tr> <tr> <td>■10⁻⁴ ÷ ■10⁻³ m/s</td> <td>7</td> </tr> <tr> <td>10⁻³ ÷ ■10⁻² m/s</td> <td>8</td> </tr> <tr> <td>■10⁻² ÷ 10⁻¹ m/s</td> <td>9</td> </tr> <tr> <td>10⁻¹ m/s</td> <td>10</td> </tr> </tbody> </table> | Hydraulic conductivity | Score | 10 ⁻⁶ m/s | 4 | ■10 ⁻⁶ - 10 ⁻⁵ m/s | 5 | 10 ⁻⁵ ÷ 10 ⁻⁴ m/s | 6 | ■10 ⁻⁴ ÷ ■10 ⁻³ m/s | 7 | 10 ⁻³ ÷ ■10 ⁻² m/s | 8 | ■10 ⁻² ÷ 10 ⁻¹ m/s | 9 | 10 ⁻¹ m/s | 10 | <p>f)</p> <table style="width: 100%; border-collapse: collapse;"> <thead> <tr> <th>Score</th> </tr> </thead> <tbody> <tr> <td>< 2 %</td> </tr> <tr> <td>2 %÷5 %</td> </tr> <tr> <td>_____</td> </tr> </tbody> </table> | Score | < 2 % | 2 %÷5 % | _____ | | | | | | | | | | | | | | | | |
| Hydraulic conductivity | Score | | | | | | | | | | | | | | | | | | | | | | | | | | | | | | | | | | | | |
| 10 ⁻⁶ m/s | 4 | | | | | | | | | | | | | | | | | | | | | | | | | | | | | | | | | | | | |
| ■10 ⁻⁶ - 10 ⁻⁵ m/s | 5 | | | | | | | | | | | | | | | | | | | | | | | | | | | | | | | | | | | | |
| 10 ⁻⁵ ÷ 10 ⁻⁴ m/s | 6 | | | | | | | | | | | | | | | | | | | | | | | | | | | | | | | | | | | | |
| ■10 ⁻⁴ ÷ ■10 ⁻³ m/s | 7 | | | | | | | | | | | | | | | | | | | | | | | | | | | | | | | | | | | | |
| 10 ⁻³ ÷ ■10 ⁻² m/s | 8 | | | | | | | | | | | | | | | | | | | | | | | | | | | | | | | | | | | | |
| ■10 ⁻² ÷ 10 ⁻¹ m/s | 9 | | | | | | | | | | | | | | | | | | | | | | | | | | | | | | | | | | | | |
| 10 ⁻¹ m/s | 10 | | | | | | | | | | | | | | | | | | | | | | | | | | | | | | | | | | | | |
| Score | | | | | | | | | | | | | | | | | | | | | | | | | | | | | | | | | | | | | |
| < 2 % | | | | | | | | | | | | | | | | | | | | | | | | | | | | | | | | | | | | | |
| 2 %÷5 % | | | | | | | | | | | | | | | | | | | | | | | | | | | | | | | | | | | | | |
| _____ | | | | | | | | | | | | | | | | | | | | | | | | | | | | | | | | | | | | | |

Tab. 1 - Classifying tables used for score assignment: a) depth to water; b) actual infiltration; c) soil media; d) aquifer media characteristics; e) hydraulic conductivity; f) slope gradient.

| parameter | severe impact | seepage | karst | fissured |
|-----------|---------------|----------|----------|----------|
| S | 5 | 4 | 2 | 3 |
| I | 5 | 4 | 5 | 3 |
| N | 4 | 4 | 1 | 3 |
| T | 5 | 2 | 3 | 4 |
| A | 3 | 5 | 5 | 4 |
| C | 2 | 5 | 5 | 5 |
| S | 2 | 2 | 5 | 4 |

Tab. 2 - Set of weights used for vulnerability assessment.

in the southern zone. The depth to water increases toward the coastline in the NE.

The actual infiltration map was computed on the basis of climatic and hydrologic data. The precipitation and temperature data were acquired in three gauges located within or in the neighborhood of the study area: Adelfia (151 m a.s.l.), Casamassima (223 m a.s.l.) and Turi (250 m a.s.l.). The net precipitation **Q** was computed by applying the **Thornthwaite-Mather** method (1957). The hydraulic characteristics of the **terrain** were analyzed using the DTM. The drainage pattern was computed automatically using simple neighborhood functions available in the GIS. The digital map of the drainage pattern was combined with the interpolated map of net precipitation to produce an actual infiltration map. The resulting mean value of actual infiltration over the whole area is 112 mm/year, with minimum and maximum values of 86 mm/year and 176 mm/year respectively.

To evaluate the contribution of the unsaturated zone, firstly its thickness was calculated by overlaying the interpolated maps of soil thickness and depth to water. The unsaturated zone thickness was normalized to 1 and combined with a weighted geological map in order to consider the variations in permeability and porosity of the different geological units. The unsaturated zone effect scores for the different geological units ranged between 2 and 3 for the alluvial deposits, 3 and 4 for the calcarenite and 4 and 8 for the limestone.

In the study area there is a high correlation between geology and soil characteristics. Over the Mesozoic limestone a discontinuous thin layer of clay soil is present. A loam to clay soil of thickness between 50 and 150 cm covers the calcarenite deposits. Thick layers of clay soil are present along the valleys and in the **dolines**. The geological map was used to assign the scores for the soil variable (table 1 c).

The maps of hydraulic conductivity and saturated zone thickness were reclassified and combined together to produce a score map of aquifer media characteristics (table 1 d).

The hydraulic conductivity map was derived from the map computed by interpolation of values measured in piezometers and wells. Due to the karst nature of the aquifer, the hydraulic conductivity values are medium-low in average with high variability in space.

The slope gradient was calculated by the first derivative of the elevation value of the

DTM. The steepest gradient in the area is 37% on the gouge slopes. The highest score of 10 was assigned to the flat areas of 0% slope gradient (table 1 f).

A set of scores was assigned to all the variables used for the SINTACS method. In order to do so the interpolated maps were reclassified using the classification tables reported in tabel. In fig. 3 the score map of hydraulic conductivity is shown as an example.

The local hydrogeological setting and impact of human activities can be classified into four of the different categories defined in the SINTACS method: severe impact, seepage, karst and fissured (Civita & De Maio, 1997). For each of these categories a different set of weights were used (table 2). The urban and industrial areas were classified as "severe impact", the drainage network as "seepage", the dolines and quarries and their surroundings as "karst", and all the other areas as "fissured". A digital map representing the spatial distribution of these categories was produced in the GIS.

The computing of the final intrinsic vulnerability map was carried out by a digital overlay process of the different variable maps and the SINTACS categories map (fig. 4). The vulnerability values, in percentage, were then classified in qualitative vulnerability categories as defined in the SINTACS method. The output digital vulnerability map is shown in fig. 5.

Conclusions

The intrinsic vulnerability map produced using the GIS approach reports the presence of four vulnerability classes in the study area: low, medium, high and very high. Most of the area is classified as highly vulnerable. Very high risk is reported where karst features are present on the terrain (dolines) or the hydrodynamic characteristics of the aquifer make it particularly vulnerable. The urban areas are generally classified as medium vulnerable.

In general, this map reports a moderately lower grade of vulnerability than in the study accomplished by Cotecchia et al. (1999b). In fact, the low vulnerability class was not present in their map while some small areas were classified as extremely high. Comparing the vulnerability at each point, it can be observed that these small differences are mainly due to the different spatial resolutions used in the two studies (10 m and 500 m). Furthermore the methods used to assign the scores to each variable in this study generally appear to guarantee a more prudent vulnerability evaluation. The two vulnerability maps are substantially similar despite the slightly lower vulnerability values in this study.

The results of this study confirm the high vulnerability of the groundwater in the Murgia acquifer. The intrinsic vulnerability map produced can provide useful information with sufficient spatial resolution and precision for the planning of local human activities.

References

- AA.VV. (1993) – Studi sulla vulnerabilità degli acquiferi – Pitagora Ed., Vol.1-2, Bologna.
Ciaranfi N., Pieri P., Ricchetti G. (1988) – Note alla carta geologica delle Murge e del Salento (Puglia centromeridionale)– Mem. Soc. Geol. It., 41,449-460, 1 tav., Rome.

- Civita M. & De Maio M. (1997) – S.I.N.T.A.C.S. un sistema parametrico per la valutazione e la cartografia della vulnerabilità degli acquiferi all'inquinamento – Pitagora Ed., Bologna.
- Civita M. (1987) – La previsione e la prevenzione del rischio d'inquinamento delle acque sotterranee a livello regionale mediante le carte di vulnerabilità – Atti Conv. Inq. Acque Sotterranee, 9-17, Mantova.
- Civita M. (1994) – Le carte della vulnerabilità degli acquiferi all'inquinamento – Pitagora Ed., Bologna.
- Cotecchia V. (1977) - Studi e ricerche sulle acque sotterranee e sull'intrusione marina in Puglia (Penisola Salentina). *Quaderni dell'Istituto di Ricerca sulle Acque*, 20, 1-466.
- Cotecchia V., Daurh M, Limoni P.P., Mitolo D., Polemio M. (1999a) - La vulnerabilità intrinseca di un'area campione dell'acquifero della Murgia (Puglia). *Pubbl. GNDCI n. 2007, III Conv. Naz. Sulla Protezione e Gestione delle Acque Sotterranee per il III Millennio*, 1.11-1.20, 13-15/10/1999, Parma.
- Cotecchia V., Daurh M, Limoni P.P., Mitolo D., Polemio M. (1999b) – Carta della Vulnerabilità dell'acquifero murgiano; Area campione a Sud-Est di Bari. – *Pubbl. GNDCI n.1964, Atti del 3° Conv. Naz. sulla Protez. e Gest. delle Acque Sotterranee per il III Millennio*, Parma.
- Grassi D. (1973) - Fondamentali aspetti dell'idrogeologia carsica della Murgia (Puglia), con particolare riferimento al versante adriatico. *Geol. Appl. e Idrogeol.*, VIII, 2, 285-313.
- Provincia di Bari (1999) – Studio per la realizzazione di una carta pedologica di sintesi e di carte derivate applicative per il territorio della Provincia di Bari. – Provincia di Bari, Assessorato all'Agricoltura, Tecnomack, Bari.
- Ricchetti G. (1975) – Nuovi dati stratigrafici sul Creatacco delle Murge, emersi da indagini nel sottosuolo. – *Boll. Soc. Geol. It.*, 94, 1083-1108, Roma.
- Ricchetti G. (1980) – Contributo alla conoscenza strutturale della Fossa Bradanica e delle Murge. – *Boll. Soc. Geol. It.*, 99,421-430, Roma.
- Thornthwaite C.W. & Mather J.R. (1957) – Instructions and tables for computing potential evapotranspiration and the water balance. *Pubbl. Clim. Drexel Ins. Technol.*, 10.
- Valduga A. (1965) – Contributo alla conoscenza geologica delle Murge baresi. – *Studi Geol. e Morf. sulla Rcg. Pugliese*, 1, 26 pp., Bari.